THE JOURNAL OF BIOLOGICAL CHEMISTRY VOL. 286, NO. 10, pp. 8158–8164, March 11, 2011

Distortion of tRNA upon Near-cognate Codon Recognition on the Ribosome*

Received for publication, December 7, 2010, and in revised form, January 5, 2011 Published, JBC Papers in Press, January 6, 2011, DOI 10.1074/jbc.M110.210021

Joerg Mittelstaet, Andrey L. Konevega, and Marina V. Rodnina[1]

From the Department of Physical Biochemistry, Max-Planck-Institute for Biophysical Chemistry, Am Fassberg 11, 37077 Göttingen, Germany

The accurate decoding of the genetic information by the ribosome relies on the communication between the decoding center of the ribosome, where the tRNA anticodon interacts with the codon, and the GTPase center of EF-Tu, where GTP hydrolysis takes place. In the A/T state of decoding, the tRNA undergoes a large conformational change that results in a more open, distorted tRNA structure. Here we use a real-time transient fluorescence quenching approach to monitor the timing and the extent of the tRNA distortion upon reading cognate or near-cognate codons. The tRNA is distorted upon codon recognition and remains in that conformation until the tRNA is released from EF-Tu, although the extent of distortion gradually changes upon transition from the pre- to the post-hydrolysis steps of decoding. The timing and extent of the rearrangement is similar on cognate and near-cognate codons, suggesting that the tRNA distortion alone does not provide a specific switch for the preferential activation of GTP hydrolysis on the cognate codon. Thus, although the tRNA plays an active role in signal transmission between the decoding and GTPase centers, other regulators of signaling must be involved.

Proteins are synthesized from aminoacyl-tRNAs (aa-tRNAs)[2] that are delivered to the ribosome in ternary complexes with elongation factor Tu (EF-Tu) and GTP. The ribosome selects aa-tRNAs according to the sequence of codons in the mRNA template and rejects the bulk of aa-tRNAs with anticodons that do not match the given codon in each round of elongation. Correct base pairing between the mRNA codon and the anticodon of the tRNA on the 30S subunit of the ribosome provides a signal that is then transmitted to the GTPase center of EF-Tu on the 50S subunit and results in the activation of GTP hydrolysis by EF-Tu. Mismatches in the codon-anticodon complex impair GTPase activation, thereby allowing the ribosome to reject incorrect ternary complexes prior to GTP hydrolysis. Deciphering the mechanism and the specificity of signal transmission between the decoding center and the GTPase center of EF-Tu is one of the central questions in understanding the fidelity of translation.

Decoding entails a number of elemental steps. Initial binding of the ternary complex EF-Tu·GTP·aa-tRNA to the ribosome takes place codon-independently, mainly through contacts of EF-Tu with ribosomal protein L7/12, and is followed by rapid and reversible codon reading (Fig. 1*A*; reviewed in Refs. 1–4). The formation of the fully complementary codon-anticodon duplex induces local and global conformational changes at the decoding center of the ribosome, which lock the aa-tRNA in the codon-bound state and activate EF-Tu for rapid GTP hydrolysis (5–8). Binding of near-cognate ternary complexes that entail single mismatches between codon and anticodon does not induce these structural rearrangements or rapid GTP hydrolysis, explaining why initial tRNA selection is more accurate than can be accounted for by the energetic differences between fully matched and mismatched codon-anticodon pairs alone. Hydrolysis of GTP and dissociation of inorganic phosphate (P_i) leads to a conformational rearrangement of EF-Tu, which is followed by the release of aa-tRNA from EF-Tu·GDP and the dissociation of the factor from the ribosome (9). Aa-tRNA is then either accommodated in the peptidyl transferase center or rejected in a proofreading mechanism.

Following codon recognition and prior to the release from EF-Tu, the aa-tRNA is bound in the so-called A/T state in which it transiently assumes a conformation that is more open or distorted compared with the unbound tRNA (10–15). The timing or the exact step at which the tRNA changes the conformation is not known. The important role of the tRNA distortion is to pull EF-Tu into its productive, GTPase-activated conformation (12, 13). It is attractive to speculate that the tRNA distortion might be a key regulator of signaling between the decoding site and the GTP binding site of EF-Tu. Mismatches in the codon-anticodon complex might impair or abrogate the tRNA distortion; as a result, the GTPase conformation of EF-Tu would not be induced; hence the slow GTP hydrolysis in a near-cognate complex. In fact, the physical properties of the tRNA body are important for accurate decoding (16–19), which would be in line with the model.

The structural details of the tRNA distortion and the concomitant rearrangements of EF-Tu that take place upon reading a correct codon on the ribosome are well-documented (10–15). However, the conformation of the tRNA reading a near-cognate codon is not known. Here we compare the formation of the transient distorted tRNA intermediate upon reading cognate or near-cognate codons. We took advantage of a rearrangement in the D stem of aa-tRNA resulting in the ~5 Å displacements in the distorted tRNA in the A/T state on a cognate codon (12). A fluorescence reporter group, proflavin, inserted at positions 16/17 in the D loop produces a fluorescent signal upon codon recognition (20). The effect can be explained

* This work was supported by the Deutsche Forschungsgemeinschaft.
[1] To whom correspondence should be addressed: Dept. of Physical Biochemistry, Max-Planck-Institute for Biophysical Chemistry, Am Fassberg 11, 37077 Göttingen, Germany. Tel.: 49-0551-2012901; Fax: 49-0551-2012905; E-mail: rodnina@mpibpc.mpg.de.
[2] The abbreviation used is: aa-tRNA, aminoacyl-tRNA.

by partial unstacking of proflavin from the neighboring guanines at positions 15 and 18 (20), which releases the fluorophore from static quenching (21), probably caused by photoinduced electron transfer between the fluorophore and the guanines (22). The distortion increases the accessibility of the proflavin reporter group for fluorescence quenchers such as iodide ions (20), consistent with a more open structure in the D arm region of the aa-tRNA (10–13). Here we study the time-resolved distortion of aa-tRNA at different stages of decoding on cognate and near-cognate codons by monitoring the transient fluorescence quenching in real time.

EXPERIMENTAL PROCEDURES

Biochemical Procedures—All experiments were carried out in buffer A (similar to HiFi (5)) (50 mM Tris-HCl, pH 7.5, 50 mM NH_4Cl, 50 mM KCl, 3.5 mM $MgCl_2$, 0.5 mM spermidine, 8 mM putrescine, 2 mM DTT) at 20 °C, if not stated otherwise. Titrations with fluorescence quencher were done in buffer A containing KI (suprapur grade, Merck) as indicated and KCl, keeping the concentration of KI + KCl constant at 150 mM. Buffer B (50 mM Tris-HCl, pH 7.5, 100 mM NH_4Cl, 7 mM $MgCl_2$) was used for the preparation of initiation and ternary complexes. Ribosomes, EF-Tu, and fMet-tRNA^{fMet} from *Escherichia coli* were prepared as described (5, 20, 23, 24). The mRNAs (28 nucleotides long) with a UUC (cognate) or CUC (near-cognate) codon following the AUG start codon were purchased from Microsynth.

The preparation of proflavin-labeled yeast tRNA^{Phe} proceeds in two steps: reduction of the dihydroU base at position 16/17 in the D loop by borohydride treatment followed by the attachment of proflavin (21). tRNA^{Phe} (10 A_{260} units/ml in 0.2 M Tris-HCl (pH 7.5)) was mixed with $NaBH_4$ solution (100 mg in 1 ml of KOH). After incubation for 30 min at 0 °C in the dark, the reaction was stopped by the addition of acetic acid to pH 4–5, and the tRNA was precipitated with cold ethanol and 0.3 M potassium acetate (pH 4.5). Ethanol precipitation was repeated 3–4 times to remove traces of borohydride. Proflavin labeling was carried out by adding borohydride-treated tRNA^{Phe} to 3 mM proflavin in 0.1 M sodium acetate pH 4.3. After incubation for 2 h at 37 °C in the dark, the reaction was stopped by the addition of 1 M Tris-HCl (pH 9) to pH 7.5. Free dye was removed by phenol extraction and ethanol precipitation. Incorporation of proflavin was quantified photometrically by measuring absorbance at 260 nm and 460 nm. For fully labeled tRNA, the A_{460}:A_{260} ratio is 0.055.

Initiation complexes were formed in buffer B by incubating ribosomes (1 μM), mRNA (3 μM), f[^{3}H]Met-tRNA^{fMet} (1.5 μM), IF1, IF2, IF3 (1.5 μM each), and GTP (1 mM) for 1 h at 37 °C, and purified by centrifugation through a 1.1 M sucrose cushion in buffer B (400 μl) for 2 h at 259,000 × *g* in a Beckmann Optima Max-XP ultracentrifuge at 4 °C. After centrifugation, pellets were dissolved in buffer B, shock-frozen in liquid nitrogen and stored at −80 °C. Ternary complex EF-Tu·GTP·[^{14}C]Phe-tRNA^{Phe}(Prf) was prepared by incubating EF-Tu (wild-type or H84A mutant) (50 μM), GTP (1 mM), phosphoenolpyruvate (3 mM), pyruvate kinase (0.05 mg/ml), tRNA^{Phe}(Prf) (25 μM), CTP (1 mM), ATP (3 mM), [^{14}C]phenylalanine (40 μM), nucleotidyl-terminal transferase and phenylalanyl-tRNA synthetase (0.5% v/v each) in buffer B containing 20 mM $MgCl_2$ and purified by gel filtration on 2× Superdex 75 HR columns (GE Healthcare) in buffer B. Ternary complex and initiation complexes were adjusted to buffer A immediately before the experiments.

Kinetic Measurements—Fluorescence stopped-flow experiments were performed using a SX-20MV apparatus (Applied Photophysics, Leatherhead, UK), monitoring proflavin fluorescence. Excitation was at 463 nm and the fluorescence was measured after passing a 500-nm cutoff filter (KV 500, Schott). Time courses were measured at pseudo-first-order conditions in excess of initiation complexes (1 μM) over ternary complexes (0.2 μM) and were evaluated by fitting an exponential function, $F = F_\infty + A \times \exp(-k_{app} \times t)$. If necessary, additional exponential terms were included. The differential amplitudes obtained at different KI concentrations were fitted according to the Stern-Volmer equation in the form of Equation 1,

$$A_0 - A = A_0 \times (1 - 1/(1 + K_{SV} \times [KI])) \qquad \text{(Eq. 1)}$$

to yield Stern-Volmer constants, K_{SV}, for collisional quenching. Steady-state fluorescence measurements were carried out in a Fluorolog-3 (Horiba Jobin Yvon) spectrofluorimeter. Excitation was at 463 nm and the emission was measured at 502 nm; the K_{SV} values were calculated as described (25).

Calculations were performed using TableCurve (Jandel Scientific) or Prism (Graphpad Software). Modeling of reaction intermediates was performed in Scientist (Micromath) based on the following kinetic scheme in Equation 2,

$$IC + TC \underset{k_{-1}}{\overset{k_1}{\rightleftharpoons}} A \underset{k_{-2}}{\overset{k_2}{\rightleftharpoons}} B \xrightarrow{k_3} C \xrightarrow{k_4} D \begin{array}{l} \xrightarrow{k_5} E \\ \searrow^{k_7} F \end{array} \qquad \text{(Eq. 2)}$$

where ternary complex (*TC*) and initiation complex (*IC*) form the initial binding complex *A*, which is converted to codon recognition complex *B*. *C* represents the state after GTPase activation and GTP hydrolysis, *D* the state after phosphate release from EF-Tu, and *E* the state after accommodation of the aa-tRNA into the *A* site. *F* represents the proofreading pathway, in which aa-tRNA is rejected from the ribosome. For the cognate ternary complex, the following rate constants were used: k_1 = 140 $\mu M^{-1}\,s^{-1}$ and $k_{-1} = 85\ s^{-1}$ for initial binding, $k_2 = 190\ s^{-1}$ and $k_{-2} = 0.23\ s^{-1}$ for codon recognition, $k_3 = 260\ s^{-1}$ for GTPase activation and GTP hydrolysis and $k_5 = 23\ s^{-1}$ for the accommodation and peptide bond formation (5). The rate of P_i release ($k_4 = 10\ s^{-1}$, data not shown) was measured for the present conditions as described (9). For the near-cognate ternary complexes, $k_1 = 140\ \mu M^{-1}\,s^{-1}$, $k_{-1} = 85\ s^{-1}$, $k_2 = 190\ s^{-1}$, $k_{-2} = 80\ s^{-1}$, and $k_3 = 0.1\ s^{-1}$ were used (Ref. 5 and data not shown). The k_5 and k_7 values for the accommodation and rejection of the near-cognate tRNA could not be determined at HiFi conditions, because the GTPase activation is strongly rate limiting. Because the efficiency of proofreading is essentially the same in HiFi (5) and the buffer with 10 mM Mg^{2+} (8), the values from the latter work were used, $k_5 = 0.1\ s^{-1}$ and $k_7 = 6\ s^{-1}$. The concentration of IC and TC used for modeling were the same as in the biochemical experiments, 1 μM and 0.2 μM, respectively.

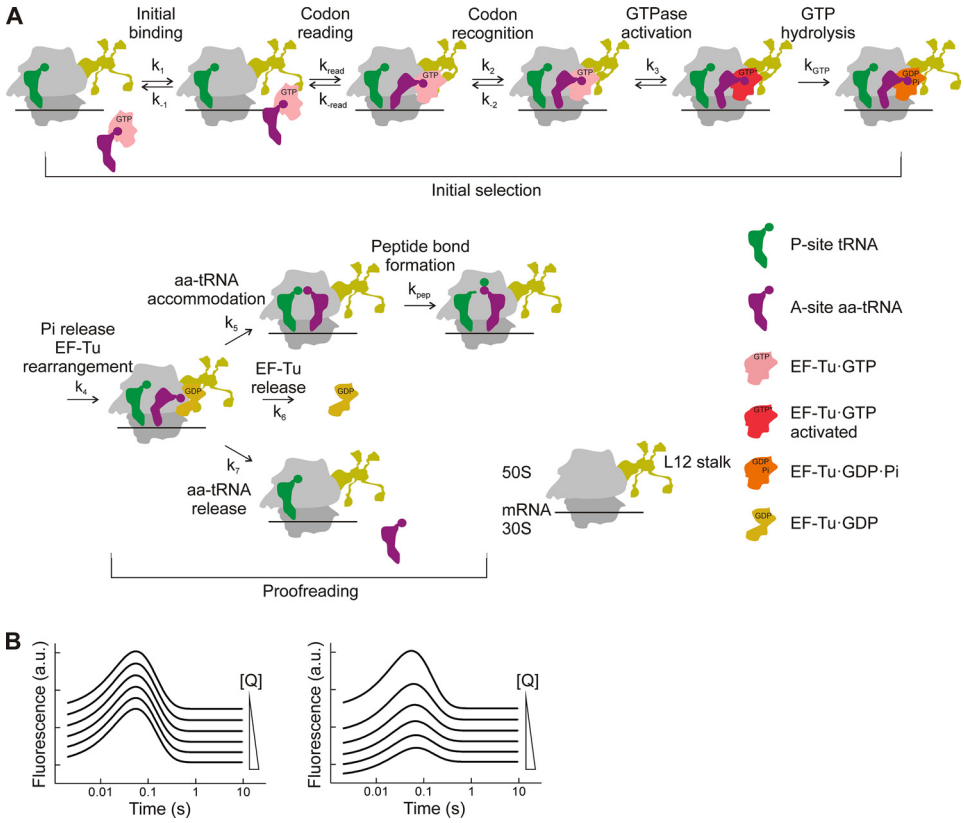

FIGURE 1. **Experimental setup.** *A*, schematic of EF-Tu-dependent aa-tRNA binding to the A site. Kinetically resolved steps are indicated by the rate constants k_1 to k_7 (forward reactions) and k_{-1} and k_{-2} (backward reactions). The rate of codon reading (presumably a readily reversible step (30)) could not be determined by rapid kinetics; the values available from single-molecule FRET experiments (30, 41) are not comparable with the values given here due to differences in buffer conditions. Rate constants of the two chemical steps that are rate-limited by the respective preceding step are designated k_{GTP} and k_{pep}. *B*, possible alternative outcomes of a transient fluorescence quenching experiment. Simulated time courses indicate fluorescence changes in aa-tRNA upon decoding at increasing (*top* to *bottom*) concentration of quencher (*Q*). *Left panel*: initial, final, and transient high fluorescence states are quenched to the same extent. *Right panel*: transient intermediate is quenched more than the initial and final states.

RESULTS

Transient Fluorescence Quenching Approach—To assess the extent of tRNA distortion at the D loop, the binding of the ternary complex EF-Tu·GTP·Phe-tRNA^{Phe}(Prf) to the ribosome was followed in a stopped-flow apparatus, monitoring proflavin fluorescence in the presence of increasing concentrations of the fluorescence quencher KI, while keeping the ionic strength constant. Changes of proflavin fluorescence report the transient formation of several intermediates of decoding (20, 26). If the fluorescence in all intermediates were quenched to the same extent, then the relative amplitudes of the various kinetic steps would be expected to be the same in the presence or the absence of the quencher (Fig. 1*B*). Alternatively, if the fluorescence of a certain intermediate would be quenched more than that of other states, this would indicate a higher exposure of the fluorophore and hence a more open tRNA conformation in that intermediate. To determine the quenching constant of an intermediate, the time courses obtained in the presence of various concentrations of KI (denoted as I) are subtracted from the one obtained without quencher (I_0). The resulting differential curves ($I_0 - I$) can be deconvoluted into exponential terms which are characterized by the apparent rate constants (k_{app}) and amplitudes ($A_0 - A$) of the respective steps. To determine the Stern-Volmer quenching constant, K_{SV}, which depends on the accessibility of the fluorophore for the quencher and, therefore, is a measure for the "openness" of the tRNA, the differential amplitudes of each step were plotted against the concentration of KI, and the plots were evaluated according to the Stern-Volmer relationship (Equation 1 in "Experimental Procedures"). The transient fluorescence quenching approach is particularly suitable for the analysis of transient intermediates in rapid, forward-committed reactions, such as the EF-Tu-dependent aa-tRNA binding to the A site. Other advantages of the transient quenching approach are the possibilities (i) to isolate a distorted tRNA intermediate from the coexisting ensemble of states that are not distorted as the reaction proceeds and (ii) to selectively monitor those tRNAs that bind to the ribosome, because only those contribute to fluorescence changes.

Transient Distortions—We first monitored the changes of the tRNA conformation that take place upon reading a cognate codon. The ternary complex, EF-Tu·GTP·Phe-tRNA^{Phe}(Prf), was mixed with the ribosomal initiation complex, 70S·mRNA·fMet-tRNA^{fMet} exposing a cognate UUC codon in the A site and the changes in Prf fluorescence were monitored (Fig. 2*A*). As observed previously, the proflavin fluorescence transiently increased during the time course of the reaction. According to our previous detailed step assignment, the fluorescence increase reflects all steps starting from ternary complex binding to the ribosome up to GTPase activation (5, 20, 26) (Fig. 1*A*).

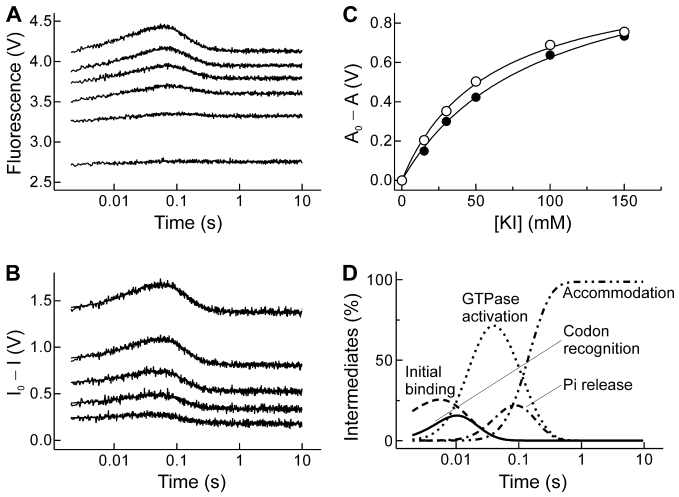

FIGURE 2. **Transient distortion of Phe-tRNA^{Phe} (Prf) upon ternary complex binding to ribosomes with a cognate UUC codon in the A site.** *A*, fluorescence change at increasing KI concentrations (*top* to *bottom*: 0, 15, 30, 50, 100, and 150 mM KI). *B*, deconvolution of intermediates. Differential curves obtained by the subtraction of the quenched traces (indicated as *I*) from the trace measured in absence of quencher (I_0) (*top* to *bottom*: $I_0 - I$ at [KI] = 150, 100, 50, 30, and 15 mM). *Solid lines* show two-exponential fits with $k_{app1} = 30\ s^{-1}$ and $k_{app2} = 10\ s^{-1}$. *C*, Stern-Volmer plots for quenching during the early (codon recognition, GTPase activation, GTP hydrolysis (Fig. 1*A*); *closed circles*) and late (post-hydrolysis steps of Fig. 1*A*; *open circles*) steps of ternary complex binding. The data were analyzed using the Stern-Volmer equation (Equation 1 in "Experimental Procedures"), and the results are summarized in Table 1. *D*, evolution of intermediate states of decoding. Time courses were modeled as described under "Experimental Procedures." The intermediates indicated are states after: initial binding (*dashed line*); codon recognition (*solid line*); GTPase activation and GTP hydrolysis (*dotted line*); P_i release and conformational change of EF-Tu (*dash-dot line*); accommodation and peptide bond formation (*dash-dot-dot*).

The decrease in fluorescence coincides with P_i release from EF-Tu following GTP hydrolysis, the release of the aa-tRNA from EF-Tu, and the subsequent accommodation of the aa-tRNA in the A site (Fig. 1*A*). When the stopped-flow experiments were carried out in the presence of KI, the fluorescence of Phe-tRNA^{Phe}(Prf) in both initial and final states was decreased due to quenching. In comparison, the fluorescence of the transient intermediate was decreased to a larger extent, indicating a higher accessibility of the fluorophore for the quencher and thus a more open tRNA intermediate (the scenario depicted in the *right panel* of Fig. 1*B*). Notably, at the highest KI concentration used, the transient fluorescence increase was no longer observed, indicating complete quenching and suggesting that the majority of the aa-tRNA assumes the distorted, more open state during the decoding of a cognate codon (see amplitudes in Table 1).

The differential curves could be accurately evaluated with a two-exponential function, accounting for the distortion of the tRNA and the relaxation back into the undistorted conformation (Fig. 2*B*). The K_{SV} values determined from the amplitudes of the distortion and relaxation steps (Fig. 2*C*) were in the range of 11–17 M^{-1}, much higher than the value of 5 M^{-1} obtained for the tRNA free in solution or in the ternary complex with EF-Tu·GTP (Table 1). Given that all individual rate constants are known (5, 27), the elemental step (Fig. 1*A*) can be identified at which tRNA changes the conformation (Fig. 2*D*). The formation of the distorted intermediate proceeds with the same rate as codon recognition, about 30 s^{-1} at the ligand concentrations

TABLE 1
Distortion of Phe-tRNA^{Phe}(Prf) upon decoding of cognate and near-cognate codons

State	Cognate		Near-cognate	
	K_{SV}	$A_0 - A$	K_{SV}	$A_0 - A$
	M^{-1}		M^{-1}	
No ribosome[a]	5.4 ± 0.2	n.a.	5.4 ± 0.2	n.a.
Initial binding[b]	7 ± 2	0.32	7 ± 2	0.32
Early steps[c]	11 ± 1	1.00	14 ± 2	0.56
Late steps[c]	17 ± 1	1.00	14 ± 2	0.08
Stalled by EF-Tu(H84A)	10 ± 1	0.46	11 ± 2	0.30
Stalled by kirromycin	16 ± 4	0.44	n.d.[d]	n.d.[d]

[a] K_{SV} in the absence of ribosomes was measured for the ternary complex EF-Tu·GTP·Phe-tRNA^{Phe}(Prf) at steady-state conditions (25); the calculation of the transient differential amplitudes $A_0 - A$ is not applicable (n.a.). The K_{SV} values for the free tRNA^{Phe}(Prf) and free proflavin are 5.3 ± 0.1 M^{-1} and 70 ± 1 M^{-1}, respectively.
[b] K_{SV} value for the initial binding complex was measured in a model system with non-programmed ribosomes (28).
[c] Early steps include pre-hydrolysis and GTP hydrolysis intermediates; late steps reflect post-hydrolysis steps (Fig. 1*A*). Distribution of intermediates is shown in Figs. 2*D* and 3*D*.
[d] n.d., complex not detectable.

used. The distorted intermediate accumulates through the early steps of decoding, *i.e.* codon recognition, GTPase activation, and GTP hydrolysis (Fig. 1*A*). The tRNA relaxation takes place at the same rate, about 10 s^{-1}, as the steps following GTP hydrolysis (Fig. 1*A*), which in the following are collectively denoted as the "late steps" of decoding, in contrast to the "early steps" at which the distorted tRNA intermediate is formed. Thus, the tRNA is distorted upon codon recognition and remains in an open conformation through the pre- and post-hydrolysis steps (Fig. 1*A*) until it is released from EF-Tu. On the other hand, the difference in the degree of tRNA distortion at the early and late states (K_{SV} values of 11 *versus* 17 M^{-1}) may suggest that the structural details of the conformational rearrangement gradually change upon transition from the early to the late steps of decoding (Fig. 2*C* and Table 1).

When analogous experiments were carried out with ribosome complexes exposing a near-cognate CUC codon, a fluorescence increase of Phe-tRNA^{Phe}(Prf) was observed followed by a very slow decrease (Fig. 3*A*). Previous analysis suggested that most of the amplitude of the fluorescence increase is due to the formation of the codon-recognition complex (Ref. 5 and below). Subsequent GTPase activation is impaired and GTP hydrolysis proceeds with a rate of about 0.1 s^{-1}, which is rate-limiting for the following steps of accommodation and proofreading that are observed as a fluorescence decrease (Fig. 3*A*). Because of slow GTPase activation, the codon-recognition complex accumulates as a high-fluorescence intermediate, and the addition of KI predominantly decreases the fluorescence of that intermediate (Fig. 3*B*). As determined from the KI dependence of the differential amplitudes (Fig. 3*C*), the K_{SV} values of the early and late steps are 14 M^{-1} (Table 1), which indicates the formation of an open tRNA intermediate also when the codon-anticodon complex contains a mismatch. Thus, upon reading a near-cognate codon, tRNA is distorted at the same step (upon codon recognition) and to an extent similar to that on a cognate codon.

Kinetic modeling based on the known kinetic constants (5) suggests that 53% of the ribosome-bound tRNA is in the codon-recognition complex (Fig. 3*D*), which is in excellent agreement

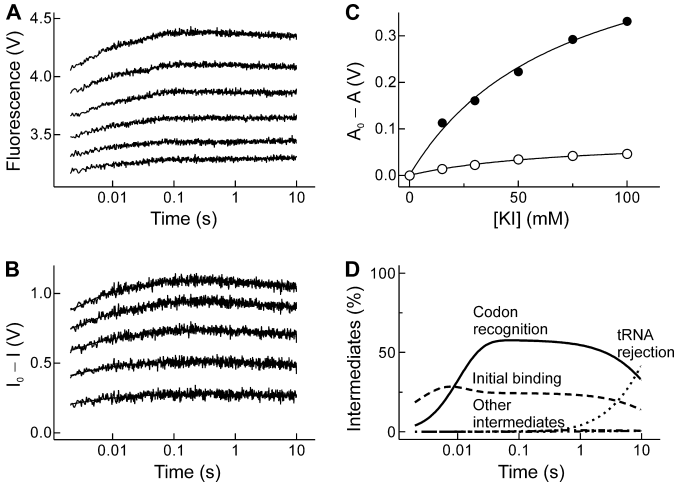

FIGURE 3. **Transient distortion of Phe-tRNA^{Phe}(Prf) upon ternary complex binding to ribosomes with a near-cognate CUC codon in the A site.** *A*, fluorescence change at increasing KI concentrations (*top* to *bottom*: 0, 15, 30, 50, 75, and 100 mM KI). *B*, deconvolution of intermediates as described in Fig. 2*B*. *C*, Stern-Volmer plots for quenching during the early (*closed circles*) and late (*open circles*) steps of ternary complex binding. The data were analyzed using the Stern-Volmer equation (Equation 1 in "Experimental Procedures") and the results are summarized in Table 1. *D*, evolution of intermediate states of decoding. Time courses were modeled as described under "Experimental Procedures." The intermediates indicated are states after: Initial binding (*dashed line*); codon recognition (*solid line*); and tRNA rejection (*dotted line*). The intermediates after GTPase activation and GTP hydrolysis (*dotted line*); P_i release and conformational change of EF-Tu (*dash-dot line*); accommodation and peptide bond formation (*dash-dot-dot*) do not accumulate.

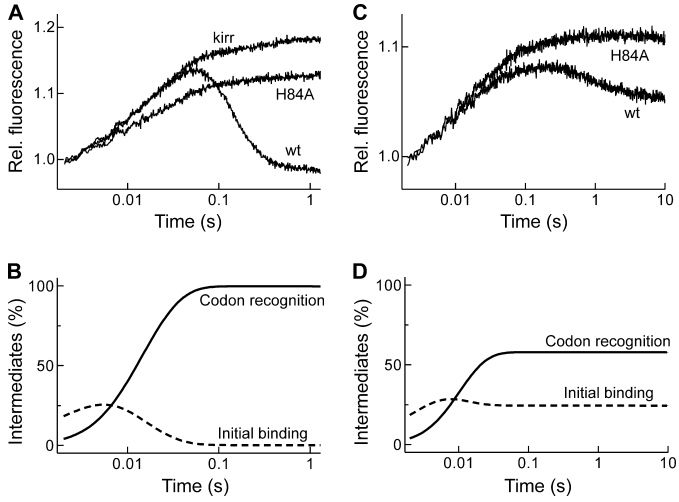

FIGURE 4. **Isolation of early and late decoding intermediates.** *A*, stalling the A/T state of cognate tRNA using mutant EF-Tu(H84A) or kirromycin (*kirr*); *wt*, wild-type EF-Tu. *B*, modeled distribution of tRNA intermediates upon decoding the cognate codon in the presence of EF-Tu(H84A). The intermediates indicated are: Initial binding (*dashed line*) and codon recognition (*solid line*); GTP hydrolysis is abolished. *C*, stalling of the near-cognate A/T state using EF-Tu(H84A). *D*, modeled distribution of the tRNA intermediates with EF-Tu(H84A) upon decoding a near-cognate codon. Intermediates are as indicated in *B*.

with the 56% fluorescence amplitude of the intermediate that is strongly quenched by KI (Table 1). From the distribution of the decoding intermediates, about 25% of aa-tRNA remains in the initial binding complex throughout the reaction (Fig. 3*D*), which may reduce the overall K_{SV} value observed for an ensemble represented by a mixture of states. Therefore, the true value of K_{SV} of either early or late steps is likely to be even higher than 14 M^{-1}. This would suggest that the tRNA distortion in the near-cognate pre-hydrolysis state may be even more extensive than in the cognate case (>14 M^{-1} compared with 11 M^{-1}). The K_{SV} values of the post-hydrolysis states are not significantly different (>14 M^{-1} and 17 M^{-1} on near-cognate and cognate codons, respectively), suggesting that the conformation of the tRNA is similar in those states.

Conformation of the tRNA in the Isolated Intermediates—To further substantiate the assignment of early and late states, we have chosen conditions at which several intermediates of A-site binding can be stalled. As a model for the initial, codon-independent binding complex, we have used EF-Tu·GTP·Phe-tRNA^{Phe}(Prf) bound to vacant ribosomes (28). The K_{SV} value of that complex, as determined by transient fluorescence quenching, 7 M^{-1} (Table 1) is in excellent agreement with the value determined at steady-state conditions.[3] The value is not much different from that of unbound or EF-Tu-bound tRNA, suggesting that in the initial binding complex the tRNA preferentially assumes a non-distorted conformation.

To stall the codon-recognition complex, GTP hydrolysis had to be inhibited. For this purpose, we utilized a mutant of EF-Tu which was impaired in GTP hydrolysis by replacing the catalytic His-84 with Ala (29). Upon binding to the cognate codon, the ternary complex EF-Tu(H84A)·GTP·Phe-tRNA^{Phe} proceeds through all steps up to codon recognition with rates similar to the wild-type complex, but is stalled prior to GTP hydrolysis (29) (Fig. 4*A*). The GTPase-activated state may be transiently sampled in this complex (29), but cannot be stabilized by the interactions of His-84 with the sarcin-ricin loop of the ribosome, as seen with the wild-type EF-Tu (13), and therefore does not accumulate. The overall amplitude of the early steps of decoding appears smaller with mutant compared with the wild-type EF-Tu (Fig. 4*A*); this can be explained by small structural differences between the A/T complexes in the pre- and post-hydrolysis states (12, 13). The K_{SV} value of the pre-hydrolysis state, as determined by the transient fluorescence quenching approach, is about 10 M^{-1}, which again indicates the aa-tRNA conformation that is more open than in the ternary complex or in free tRNA. The value is similar to that estimated for the early steps, but is somewhat lower than for the late steps of the uninterrupted decoding with wild-type EF-Tu. The contribution of the undistorted initial binding state should be relatively small in this case, as the tRNA is predominantly present in the codon-recognition state (Fig. 4*B*). This suggests that the K_{SV} = 10 M^{-1} reflects the distortion of aa-tRNA during decoding of a cognate codon. When a near-cognate codon was used, the aa-tRNA bound in the A/T complex with EF-Tu(H84A) is also distorted (Fig. 4*C*); the K_{SV} value of 11 M^{-1} is similar to that in the cognate complex (Table 1). However, because in the near-cognate case about 25% of aa-tRNA remains in the initial binding step (Fig. 4*D*), which is characterized by a lower K_{SV}, the true K_{SV} value for the near-cognate codon-recognition complex is likely >11 M^{-1}. The data suggest that in the pre-hydrolysis complex the tRNA assumes a distorted conformation, regardless of whether the A-site codon is cognate or near-cognate.

[3] M. V. Rodnina, unpublished data.

Finally, for better comparison with the structures of the complexes obtained by cryo-EM and crystallography, we also determined the K_{SV} value for aa-tRNA stalled in the A/T state by kirromycin. The antibiotic does not affect the early steps of decoding up to GTP hydrolysis and P_i release from EF-Tu, but blocks the conformational change of EF-Tu that leads to the release of aa-tRNA from the factor (9, 20). In this state, the cognate aa-tRNA is strongly distorted with a $K_{SV} = 16\ M^{-1}$ (Table 1), consistent with the value obtained for the late decoding state in full decoding. This finding further substantiates the notion that the conformation of the tRNA gradually changes toward a more open structure upon progressing from the pre- to the post-hydrolysis states. As kirromycin did not stabilize the binding of aa-tRNA on the near-cognate codon (data not shown), analogous experiments with the near-cognate A/T state were not feasible.

DISCUSSION

The Timing of tRNA Distortion—The present results suggest the following timing of the conformational rearrangements of aa-tRNA during decoding. In the ternary complex bound to the ribosome before codon reading (Fig. 1), aa-tRNA retains its undistorted, closed conformation, although transient excursions into an open conformation may occur. Upon cognate codon recognition, the tRNA assumes a conformation which is significantly more open at the D loop than in the preceding initial binding complex or in the free ternary complex with EF-Tu·GTP (Table 1). The solvent exposure of the D loop increases even further in the post-hydrolysis state up to the step when the tRNA is released from EF-Tu and accommodated in the A site (Fig. 1), which allows the tRNA to relax into the undistorted conformation. The gradual change in the tRNA arrangement between the early and late steps of decoding may reflect structural differences between the pre- and post-hydrolysis states, although the crystal structures of the tRNA in the two states are very similar (12, 13). Alternatively, as the codon-recognition step presumably entails a number of substeps and the tRNA rapidly samples between different conformations and substates (6, 7, 30), the observed solvent exposure of the given state may be a global value that represents a mixture of undistorted and distorted states. The open tRNA conformation may be favored by the contacts with the ribosome as soon as codon recognition takes place and may be further stabilized in the post-hydrolysis state.

Distortion of tRNA in the Near-cognate A/T State—The tRNA plays an important role in activation of GTP hydrolysis. An intact aa-tRNA is required for the GTPase activation of EF-Tu (18) and mutations in the D arm affect GTP hydrolysis (16, 31). The structures suggest how the tRNA distortion on a cognate codon may result in the GTPase activation of EF-Tu (12, 13). This raises the question whether the tRNA distortion provides a switch that signals the formation of a correctly matched cognate codon-anticodon complex to the GTPase center. In the simplest case, a mismatch would impair the formation of the distorted tRNA intermediate, thus precluding the structural rearrangements that are induced by cognate codon recognition and are required for GTPase activation of EF-Tu. The present data demonstrate that the formation of the open tRNA intermediate does not depend on cognate codon recognition (Table 1): When a near-cognate codon is recognized, the tRNA is distorted as well, and the timing of the rearrangements is similar to the one on the cognate codon; yet GTP hydrolysis is more than 2000-fold slower in the near-cognate compared with the cognate complex. Thus, the tRNA distortion alone does not seem to provide the specific signal for the preferential activation of GTP hydrolysis by EF-Tu in the cognate case. Additional regulators, presumably ribosome elements, must play a role in sensing and transmitting the signals that communicate the decoding to GTPase activation (see below).

In a more complicated scenario the details of the distortion may be different on the cognate and near-cognate codons, thereby affecting the GTPase activation in different ways. Given the similarity of the quenching constants of the distorted intermediates formed on cognate and near-cognate codons, large differences in the respective tRNA conformations seem unlikely, although small differences cannot be excluded. The D loop of the tRNA bound on the near-cognate codon may be even slightly more open than on the cognate one (see "Results"). Structural differences in tRNA regions distant from the D loop cannot be ruled out, but seem unlikely, given the rigidity of the molecule and the coupling in rearrangements of the tRNA elbow region and the acceptor stem interacting with EF-Tu (12, 32, 33).

Consequences for GTP Hydrolysis—GTP hydrolysis proceeds through the attack of the hydrolytic water molecule on the γ-phosphate of GTP in EF-Tu. His-84 in *E. coli* EF-Tu is the active site residue that stabilizes the GTPase transition state (13, 29, 34). Upon GTPase activation on the ribosome, His-84 has to move toward the γ-phosphate, and this movement should be induced only when a correct codon-anticodon complex is formed. The tRNA distortion affects the relative orientation between tRNA and EF-Tu (10–13), which leads to subtle rearrangement in EF-Tu and stabilization of the catalytically active orientation of His-84 by A2662 of the sarcin-ricin loop of 23S rRNA (13), thereby ultimately resulting in GTPase activation. The mechanism of activation must be precisely tuned for each cognate aa-tRNA, as all of them exhibit similar kinetic properties despite a wide variety of structural features (35). Similarly, any mismatch in the codon-anticodon complex impairs GTPase activation, regardless of the thermodynamic stability of the respective codon-anticodon complexes or their docking partners at the decoding site (27). The uniformity of mismatch recognition suggests a global response mechanism, which would be consistent with the idea that all conformational changes that occur upon cognate codon recognition, including domain closure of the 30S subunit, distortions of the tRNA, and rearrangements in EF-Tu, are essential for the precise positioning of the GTPase center of EF-Tu at the sarcin-ricin loop. Although the tRNA is distorted also in the near-cognate A/T state, even subtle changes in the orientation of tRNA and EF-Tu could cause defects in the GTPase activation by preventing A2662 from properly placing His-84 into the active site (13). In this framework, the tRNA mutants that activate GTP hydrolysis on a near-cognate codon (16, 19) appear to have found their own unique conformational solution to dock EF-Tu on the sarcin-ricin loop. However, other contacts in the decoding com-

plex may specifically affect the stringency of decoding, *e.g.* helix 14 and helix 8 of 16S rRNA that negatively regulate GTP hydrolysis (36), or the interactions between helix 5 and domain 2 of EF-Tu (37). The structural basis for the very strong effect of ribosomal protein L7/12 on the GTPase activity of EF-Tu (38, 39) remains to be clarified. Finally, the ribosome may play an active role in monitoring the correct codon-anticodon interaction using a network of rRNA and proteins from both ribosomal subunits, as suggested by the recent crystal structure of the proofreading complex (40). Further experiments will be necessary to determine the role of each interaction element in the A/T state in the codon-specific control of the GTPase activation of EF-Tu.

Acknowledgments—We thank Wolfgang Wintermeyer for critical reading the manuscript, Sandra Kappler for expert technical assistance, and David A. Tirrell (California Institute of Technology) for providing the plasmid pQE32-FRS-sc encoding for the His_6-tagged phenylalanyl-tRNA synthetase from Saccharomyces cerevisiae.

REFERENCES

1. Rodnina, M. V., Gromadski, K. B., Kothe, U., and Wieden, H. J. (2005) *FEBS Lett.* **579,** 938–9342
2. Rodnina, M. V., and Wintermeyer, W. (2001) *Annu. Rev. Biochem.* **70,** 415–435
3. Schmeing, T. M., and Ramakrishnan, V. (2009) *Nature* **461,** 1234–1242
4. Zaher, H. S., and Green, R. (2009) *Cell* **136,** 746–762
5. Gromadski, K. B., and Rodnina, M. V. (2004) *Mol. Cell* **13,** 191–200
6. Ogle, J. M., Brodersen, D. E., Clemons, W. M., Jr., Tarry, M. J., Carter, A. P., and Ramakrishnan, V. (2001) *Science* **292,** 897–902
7. Ogle, J. M., Murphy, F. V., Tarry, M. J., and Ramakrishnan, V. (2002) *Cell* **111,** 721–732
8. Pape, T., Wintermeyer, W., and Rodnina, M. (1999) *EMBO J.* **18,** 3800–3807
9. Kothe, U., and Rodnina, M. V. (2006) *Biochemistry* **45,** 12767–12774
10. Schuette, J. C., Murphy, F. V., 4th, Kelley, A. C., Weir, J. R., Giesebrecht, J., Connell, S. R., Loerke, J., Mielke, T., Zhang, W., Penczek, P. A., Ramakrishnan, V., and Spahn, C. M. (2009) *EMBO J.* **28,** 755–765
11. Villa, E., Sengupta, J., Trabuco, L. G., LeBarron, J., Baxter, W. T., Shaikh, T. R., Grassucci, R. A., Nissen, P., Ehrenberg, M., Schulten, K., and Frank, J. (2009) *Proc. Natl. Acad. Sci. U.S.A.* **106,** 1063–1068
12. Schmeing, T. M., Voorhees, R. M., Kelley, A. C., Gao, Y. G., Murphy, F. V., 4th, Weir, J. R., and Ramakrishnan, V. (2009) *Science* **326,** 688–694
13. Voorhees, R. M., Schmeing, T. M., Kelley, A. C., and Ramakrishnan, V. (2010) *Science* **330,** 835–838
14. Stark, H., Rodnina, M. V., Wieden, H. J., Zemlin, F., Wintermeyer, W., and van Heel, M. (2002) *Nat. Struct. Biol.* **9,** 849–854
15. Valle, M., Sengupta, J., Swami, N. K., Grassucci, R. A., Burkhardt, N., Nierhaus, K. H., Agrawal, R. K., and Frank, J. (2002) *EMBO J.* **21,** 3557–3567
16. Cochella, L., and Green, R. (2005) *Science* **308,** 1178–1180
17. Schultz, D. W., and Yarus, M. (1994) *J. Mol. Biol.* **235,** 1381–1394
18. Piepenburg, O., Pape, T., Pleiss, J. A., Wintermeyer, W., Uhlenbeck, O. C., and Rodnina, M. V. (2000) *Biochemistry* **39,** 1734–1738
19. Ledoux, S., Olejniczak, M., and Uhlenbeck, O. C. (2009) *Nat. Struct. Mol. Biol.* **16,** 359–364
20. Rodnina, M. V., Fricke, R., and Wintermeyer, W. (1994) *Biochemistry* **33,** 12267–12275
21. Wintermeyer, W., and Zachau, H. G. (1979) *Eur. J. Biochem.* **98,** 465–475
22. Doose, S., Neuweiler, H., and Sauer, M. (2009) *Chem. Phys. Chem.* **10,** 1389–1398
23. Milon, P., Konevega, A. L., Peske, F., Fabbretti, A., Gualerzi, C. O., and Rodnina, M. V. (2007) *Methods Enzymol.* **430,** 1–30
24. Rodnina, M. V., and Wintermeyer, W. (1995) *Proc. Natl. Acad. Sci. U.S.A.* **92,** 1945–1949
25. Robertson, J. M., and Wintermeyer, W. (1981) *J. Mol. Biol.* **151,** 57–79
26. Pape, T., Wintermeyer, W., and Rodnina, M. V. (1998) *EMBO J.* **17,** 7490–7497
27. Gromadski, K. B., Daviter, T., and Rodnina, M. V. (2006) *Mol. Cell* **21,** 369–377
28. Rodnina, M. V., Pape, T., Fricke, R., Kuhn, L., and Wintermeyer, W. (1996) *J. Biol. Chem.* **271,** 646–652
29. Daviter, T., Wieden, H. J., and Rodnina, M. V. (2003) *J. Mol. Biol.* **332,** 689–699
30. Geggier, P., Dave, R., Feldman, M. B., Terry, D. S., Altman, R. B., Munro, J. B., and Blanchard, S. C. (2010) *J. Mol. Biol.* **399,** 576–595
31. Pan, D., Zhang, C. M., Kirillov, S., Hou, Y. M., and Cooperman, B. S. (2008) *J. Biol. Chem.* **283,** 18431–18440
32. Sanbonmatsu, K. Y. (2006) *Biochimie* **88,** 1075–1089
33. Whitford, P. C., Geggier, P., Altman, R. B., Blanchard, S. C., Onuchic, J. N., and Sanbonmatsu, K. Y. (2010) *RNA* **16,** 1196–1204
34. Berchtold, H., Reshetnikova, L., Reiser, C. O., Schirmer, N. K., Sprinzl, M., and Hilgenfeld, R. (1993) *Nature* **365,** 126–132
35. Ledoux, S., and Uhlenbeck, O. C. (2008) *Mol. Cell* **31,** 114–123
36. McClory, S. P., Leisring, J. M., Qin, D., and Fredrick, K. (2010) *RNA* **16,** 1925–1934
37. Vorstenbosch, E., Pape, T., Rodnina, M. V., Kraal, B., and Wintermeyer, W. (1996) *EMBO J.* **15,** 6766–6774
38. Kothe, U., Wieden, H. J., Mohr, D., and Rodnina, M. V. (2004) *J. Mol. Biol.* **336,** 1011–1021
39. Mohr, D., Wintermeyer, W., and Rodnina, M. V. (2002) *Biochemistry* **41,** 12520–12528
40. Jenner, L., Demeshkina, N., Yusupova, G., and Yusupov, M. (2010) *Nat. Struct. Mol. Biol.* **17,** 1072–1078
41. Blanchard, S. C., Gonzalez, R. L., Kim, H. D., Chu, S., and Puglisi, J. D. (2004) *Nat. Struct. Mol. Biol.* **11,** 1008–1014

Protein Synthesis and Degradation:

Distortion of tRNA upon Near-cognate Codon Recognition on the Ribosome

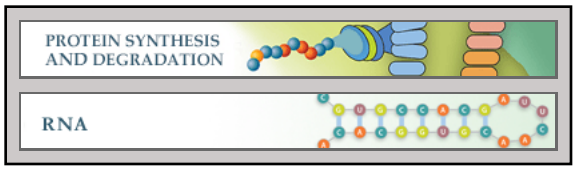

Joerg Mittelstaet, Andrey L. Konevega and Marina V. Rodnina

J. Biol. Chem. 2011, 286:8158-8164.
doi: 10.1074/jbc.M110.210021 originally published online January 6, 2011
